

AD 746512

AMPLITUDE-STABILIZED PULSED LASER

Contract No. N00014-70-C-0342

FINAL REPORT

covering the period 29 June 1970 to 29 June 1972

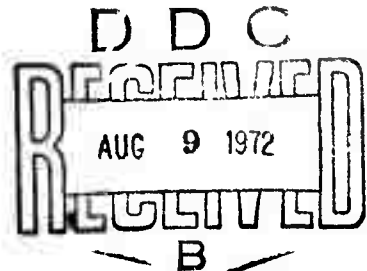
11

Wm. D. Fountain and R. L. Hansen

10 July 1972

Sponsored By
Advanced Research Projects Agency
ARPA Order No. 306

Reproduced by
NATIONAL TECHNICAL
INFORMATION SERVICE
U S Department of Commerce
Springfield VA 22151



Electro-Optics Organization
GTE Sylvania Inc.
Electronic Systems Group
Western Division
P.O. Box 188
Mountain View, California 94040

SEE AD 719931

DISTRIBUTION STATEMENT A
Approved for public release;
Distribution Unlimited

35

**BEST
AVAILABLE COPY**

DOCUMENT CONTROL DATA - R&D

(Security classification of title, body of abstract and indexing annotation must be entered when the overall report is classified)

1 ORIGINATING ACTIVITY (Corporate author) GTE Sylvania Inc. Electro-Optics Research and Development Dept. P. O. Box 188, Mountain View, Calif. 94040		2a. REPORT SECURITY CLASSIFICATION UNCLASSIFIED	
		2b. GROUP	
3 REPORT TITLE AMPLITUDE-STABILIZED PULSED LASER			
4 DESCRIPTIVE NOTES (Type of report and inclusive dates) Final Report (29 June 1970 - 29 June 1972)			
5 AUTHOR(S) (Last name, first name, initial) William D. Fountain and Ronald L. Hansen			
6 REPORT DATE 10 July 1972		7a. TOTAL NO. OF PAGES 32	7b. NO. OF REFS 12
8a. CONTRACT OR GRANT NO N00014-70-C-0342		9a. ORIGINATOR'S REPORT NUMBER(S) EOO-23	
b. PROJECT NO. ARPA Order No. 306			
c ONR Program Code No. 421		9b. OTHER REPORT NO(S) (Any other numbers that may be assigned this report)	
d			
10 AVAILABILITY/LIMITATION NOTICES Distribution of this document is unlimited			
11 SUPPLEMENTARY NOTES Administered by... Director, Physics Programs, Physical Sciences Div., Office of Naval Research Dept. of Navy, Arlington, Va.		12. SPONSORING MILITARY ACTIVITY Advanced Research Projects Agency 1400 Wilson Blvd. Arlington, Va. 22209	
13 ABSTRACT This report summarizes the results during the reporting period of a program whose goal is the development of a flash-pumped, Q-switched, mode-locked, cavity-dumped, amplitude-stabilized laser operating at approximately 1.06 μ m in the fundamental transverse (TEM ₀₀) mode. System design and test results are presented.			

Details of illustrations in this document may be better studied on microfiche

ia

14. KEY WORDS	LINK A		LINK B		LINK C	
	ROLE	WT	ROLE	WT	ROLE	WT
Nd ³⁺ laser						
mode locking						
laser amplitude stabilization						

INSTRUCTIONS

1. **ORIGINATING ACTIVITY:** Enter the name and address of the contractor, subcontractor, grantee, Department of Defense activity or other organization (*corporate author*) issuing the report.

2a. **REPORT SECURITY CLASSIFICATION:** Enter the overall security classification of the report. Indicate whether "Restricted Data" is included. Marking is to be in accordance with appropriate security regulations.

2b. **GROUP:** Automatic downgrading is specified in DoD Directive 5200.10 and Armed Forces Industrial Manual. Enter the group number. Also, when applicable, show that optional markings have been used for Group 3 and Group 4 as authorized.

3. **REPORT TITLE:** Enter the complete report title in all capital letters. Titles in all cases should be unclassified. If a meaningful title cannot be selected without classification, show title classification in all capitals in parenthesis immediately following the title.

4. **DESCRIPTIVE NOTES:** If appropriate, enter the type of report, e.g., interim, progress, summary, annual, or final. Give the inclusive dates when a specific reporting period is covered.

5. **AUTHOR(S):** Enter the name(s) of author(s) as shown on or in the report. Enter last name, first name, middle initial. If military, show rank and branch of service. The name of the principal author is an absolute minimum requirement.

6. **REPORT DATE:** Enter the date of the report as day, month, year, or month, year. If more than one date appears on the report, use date of publication.

7a. **TOTAL NUMBER OF PAGES:** The total page count should follow normal pagination procedures, i.e., enter the number of pages containing information.

7b. **NUMBER OF REFERENCES:** Enter the total number of references cited in the report.

8a. **CONTRACT OR GRANT NUMBER:** If appropriate, enter the applicable number of the contract or grant under which the report was written.

8b, 8c, & 8d. **PROJECT NUMBER:** Enter the appropriate military department identification, such as project number, subproject number, system numbers, task number, etc.

9a. **ORIGINATOR'S REPORT NUMBER(S):** Enter the official report number by which the document will be identified and controlled by the originating activity. This number must be unique to this report.

9b. **OTHER REPORT NUMBER(S):** If the report has been assigned any other report numbers (*either by the originator or by the sponsor*), also enter this number(s).

10. **AVAILABILITY/LIMITATION NOTICES:** Enter any limitations on further dissemination of the report, other than those

imposed by security classification, using standard statements such as:

- (1) "Qualified requesters may obtain copies of this report from DDC."
- (2) "Foreign announcement and dissemination of this report by DDC is not authorized."
- (3) "U. S. Government agencies may obtain copies of this report directly from DDC. Other qualified DDC users shall request through _____."
- (4) "U. S. military agencies may obtain copies of this report directly from DDC. Other qualified users shall request through _____."
- (5) "All distribution of this report is controlled. Qualified DDC users shall request through _____."

If the report has been furnished to the Office of Technical Services, Department of Commerce, for sale to the public, indicate this fact and enter the price, if known.

11. **SUPPLEMENTARY NOTES:** Use for additional explanatory notes.

12. **SPONSORING MILITARY ACTIVITY:** Enter the name of the departmental project office or laboratory sponsoring (*paying for*) the research and development. Include address.

13. **ABSTRACT:** Enter an abstract giving a brief and factual summary of the document indicative of the report, even though it may also appear elsewhere in the body of the technical report. If additional space is required, a continuation sheet shall be attached.

It is highly desirable that the abstract of classified reports be unclassified. Each paragraph of the abstract shall end with an indication of the military security classification of the information in the paragraph, represented as (TS), (S), (C), or (U).

There is no limitation on the length of the abstract. However, the suggested length is from 150 to 225 words.

14. **KEY WORDS:** Key words are technically meaningful terms or short phrases that characterize a report and may be used as index entries for cataloging the report. Key words must be selected so that no security classification is required. Identifiers, such as equipment model designation, trade name, military project code name, geographic location, may be used as key words but will be followed by an indication of technical context. The assignment of links, rules, and weights is optional.

FINAL REPORT

AMPLITUDE-STABILIZED PULSED LASER

Contract No. N00014-70-C-0342 (Office of Naval Research)

performance period 29 June 1970 to 17 April 1972

contract value: \$117,770

Order No. 306 (Advanced Research Projects Agency)


Program code No. 421 (Office of Naval Research)

Project No. 462 (GTE Sylvania, Electronic Systems Group, Western Division)

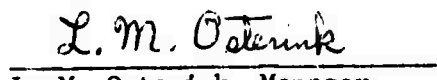
Project Engineer/Principal Investigator: Wm. D. Fountain
(415) 966-2261

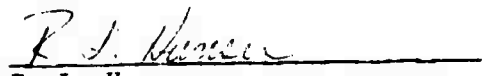
10 July 1972

Prepared by


Wm. D. Fountain
Electro-Optics Research and
Development Department,
Optically-Pumped Lasers Section

Approved by


L. M. Osterink, Manager
Electro-Optics Research and
Development Department


R. L. Hansen
Electro-Optics Research and
Development Department,
Optically-Pumped Lasers Section

Electro-Optics Organization
GTE Sylvania Inc.
Electronic Systems Group
Western Division
P.O. Box 188
Mountain View, California 94040

TABLE OF CONTENTS

<u>Section</u>	<u>Title</u>	<u>Page</u>
	FOREWORD	ii
	ABSTRACT	iii
1	INTRODUCTION	1-1
2	DESIGN APPROACH	2-1
3	OPTOMECHANICAL DESIGN	3-1
3.1	Subsidiary Oscillator	3-1
3.2	Power Oscillator	3-1
3.3	Modulator and Switches	3-2
3.4	The Laser Chassis	3-2
4	ELECTRONIC DESIGN	4-1
4.1	Laser Excitation	4-1
4.2	RF Circuitry	4-3
4.3	Logic and Timing Circuitry	4-3
4.4	Pockels Cell Drive Circuitry	4-6
4.5	System Control and Protection Circuitry	4-6
5	EXPERIMENTAL RESULTS	5-1
6	RECOMMENDATIONS	6-1
7	REFERENCES	7-1
8	GLOSSARY	8-1

LIST OF ILLUSTRATIONS

<u>Figure</u>	<u>Title</u>	<u>Page</u>
2.1	Optical Block Diagram	2-3
2.2	Electronic Block Diagram	2-4
2.3	Timing Diagram	2-5
3.1	Laser Chassis	3-3
4.1	Control Console	4-2
4.2	Delay 2	4-4
4.3	GTE Sylvania Pockels Cell Driver	4-7
5.1	Pulse-Duration Experimental Setup	5-3
5.2	Pulse Autocorrelation Scan (SHG Technique)	5-4
5-3	Reflected-Beam TPF Pulse Autocorrelation Photo	5-6
5-4	Trace of Injected Pulse	5-6

11a

FOREWORD

This Final Report on "Amplitude-Stabilized Pulsed Laser", summarizing work performed during the period 29 June 1970 to 29 June 1972, was prepared by the Electro-Optics Organization of the Western Division of the Electronic Systems Group of GTE Sylvania, Inc., under Contract N00014-70-C-0342. Wm. D. Fountain and R. L. Hansen were the principal investigators under this program; Dr. J. M. Yarborough, D. Osborn, Dr. G. A. Massey, Dr. L. M. Osterink, C. B. Hitz, J. E. Raffarin, and P. Jossi have also contributed materially to this program, and we acknowledge helpful discussions with S. E. Schwarz of the University of California at Berkeley, R. L. Carman of the Lawrence Livermore Laboratory, and D. G. Currie of the University of Maryland.

All work under this program was administered by the Director, Physics Programs, Physical Sciences Div., Office of Naval Research (ONR), Department of the Navy, Arlington, Virginia, under funding from the Advanced Research Projects Agency (ARPA). The Scientific Contracting Officer's authorized representatives were F. W. Quelle (ONR/Boston) and R. E. Behringer (ONR/Pasadena), with whom we also acknowledge discussions.

ABSTRACT

This report summarizes the results during the reporting period of a program whose goal is the development of a flash-pumped, Q-switched, mode-locked, cavity-dumped, amplitude-stabilized laser operating at approximately $1.06\text{ }\mu\text{m}$ in the fundamental transverse (TEM_{00}) mode. System design and test results are presented.

1. INTRODUCTION

The goal of this program was to design and develop a 1.06μ laser, operating reliably for long periods of time without damage, with the following specifications:

pulse rate:	10 to 30 pps
pulse duration:	≤ 100 ps
pulse energy:	≥ 50 mJ @ 10 pps
amplitude fluctuation:	$\leq 4\%$ of peak (goal: $\leq 2\%$ of peak)
integrated leakage:	$\leq 10\%$ of pulse energy
beam quality:	TEM ₀₀ mode

It is worth noting that at the minimum specified performance (10 pps, 100 ps, 50 mJ) this laser must deliver an average power of 500 mW and a peak power of 500 MW.

These specifications imply that the laser material must have properties comparable to those of $\text{Nd:Y}_3\text{Al}_5\text{O}_{12}$ (hereafter, referred to as YAG); otherwise the thermally-induced stresses, focusing, and birefringence present formidable problems. The specifications also imply that the laser must be flash-pumped and Q-switched (to obtain the pulse energy), mode-locked (to obtain the pulse duration), and cavity-dumped (to obtain the pulse-to-pulse stability). Our design approach is presented in Section 2, and the design itself is presented in Sections 3 and 4.

Section 5 is devoted to the experimental results obtained with this system. Section 6 contains our recommendations for additional work relevant to potential ultimate uses of this laser, and is followed by a list of references and a glossary of abbreviations.

2. DESIGN APPROACH

There are a number of well-known techniques for the intentional mode locking of lasers; they may generally be divided into loss modulation, phase modulation (including schemes which modulate the eigenfrequencies of the resonant cavity), self-injection, and direct injection. One criterion for choosing a technique is the effective modulation depth required, which is directly related to the time required for the laser pulse to build up from noise ($P_n \sim 10^{-13}$ W) to its peak ($P_{pk} \sim 500$ MW). The number of round trips required is approximately given by

$$G^m = P_{pk}/P_n, \quad (2-1)$$

where G is the round-trip gain and m is the number of round trips. For this system, $G \approx 10$ and therefore ≈ 22 round trips are required. This implies a very large effective modulation depth, and thus eliminates all mode-locking techniques except electro-optic loss modulation, loss modulation using a bleachable dye, and direct injection.

Electro-optic loss modulation is marginal from the standpoint of modulation depth, and is eliminated by materials considerations. This is so because only LiNbO_3 and KDP, of the commonly available quality electro-optic materials, have low RF dissipation factors, but LiNbO_3 has a low threshold for laser damage and KDP has a small electro-optic coefficient. Bleachable dyes may be useable in this type of system; however, the dye must be protected from blue and higher-energy light, must be flowed and filtered, and has a somewhat limited shelf life.

Direct injection mode locking utilizes a subsidiary low-power oscillator, mode-locked by any practical technique, pulses from which are injected into the power oscillator. The peak power of the injected pulse is $P_{inj} \sim 100$ W, so the number of round trips required for buildup is approximately

$$G^{m'} = P_{pk}/P_{inj} \quad (2-2)$$

which, for this system, yields $m' \approx 7$. During this time the noise builds up to a background of approximately

$$P_b = P_n G^{m'}, \quad (2-3)$$

so that $P_b \approx 500$ nW. Actually, we have significantly overestimated P_b by using the approximation of constant small-signal gain, since the rod inversion is severely depleted during the last few passes of the built-up injected pulse. This method of mode locking has an additional advantage over other techniques in that the subsidiary oscillator can be operated in the TEM_{00} mode with little effort, and the output of this oscillator can then be expanded to fill the effective available aperture of the power oscillator. Our embodiment of this design approach is shown in Fig. 2.1. The rhomboidal structures in the figure are low-loss four-port polarizers, the design of which is proprietary to GTE Sylvania.

The output amplitude of this system is actively stabilized. In addition, several aspects of the design promote passive stability. Refer to Figures 2.1, 2.2, and 2.3. The smaller laser rod ($\sim 0.150'' \times 70$ mm) is pumped continuously by two tungsten-iodine lamps. The Brewster's-angle fused silica polarizer, the acousto-optic mode-locking modulator (ML), and the aperture constrain the rod to oscillate quasi-continuously in a polarized, mode-locked, Gaussian beam. Generally, this optical signal can be available outside the laser for timing and/or diagnostic purposes. The larger laser rod ($\sim 0.250'' \times 3''$) is flash-pumped by two Kr lamps. This rod is inverted at the end of the lamp pulse since the "Q-switch" (QS)/"rotator" (rot.) Pockels cell is at $V_{\lambda/4}$ while the "cavity-dump" (CD) Pockels cell is at zero. At this time, "switch No. 1" is switched and a mode-locked pulse is coupled into the larger rod. This pulse has its polarization rotated so that it can build up, after which time the "Q-switch/rotator" is switched to zero. Meanwhile, "switch No. 2" is switched to prevent coupling of additional mode-locked pulses and to provide protective isolation (so that any energy cross-coupled into the "wrong" polarization in the large rod does not disturb the mode-locking or damage any components in the subsidiary oscillator. When the intensity of the pulse, as monitored by

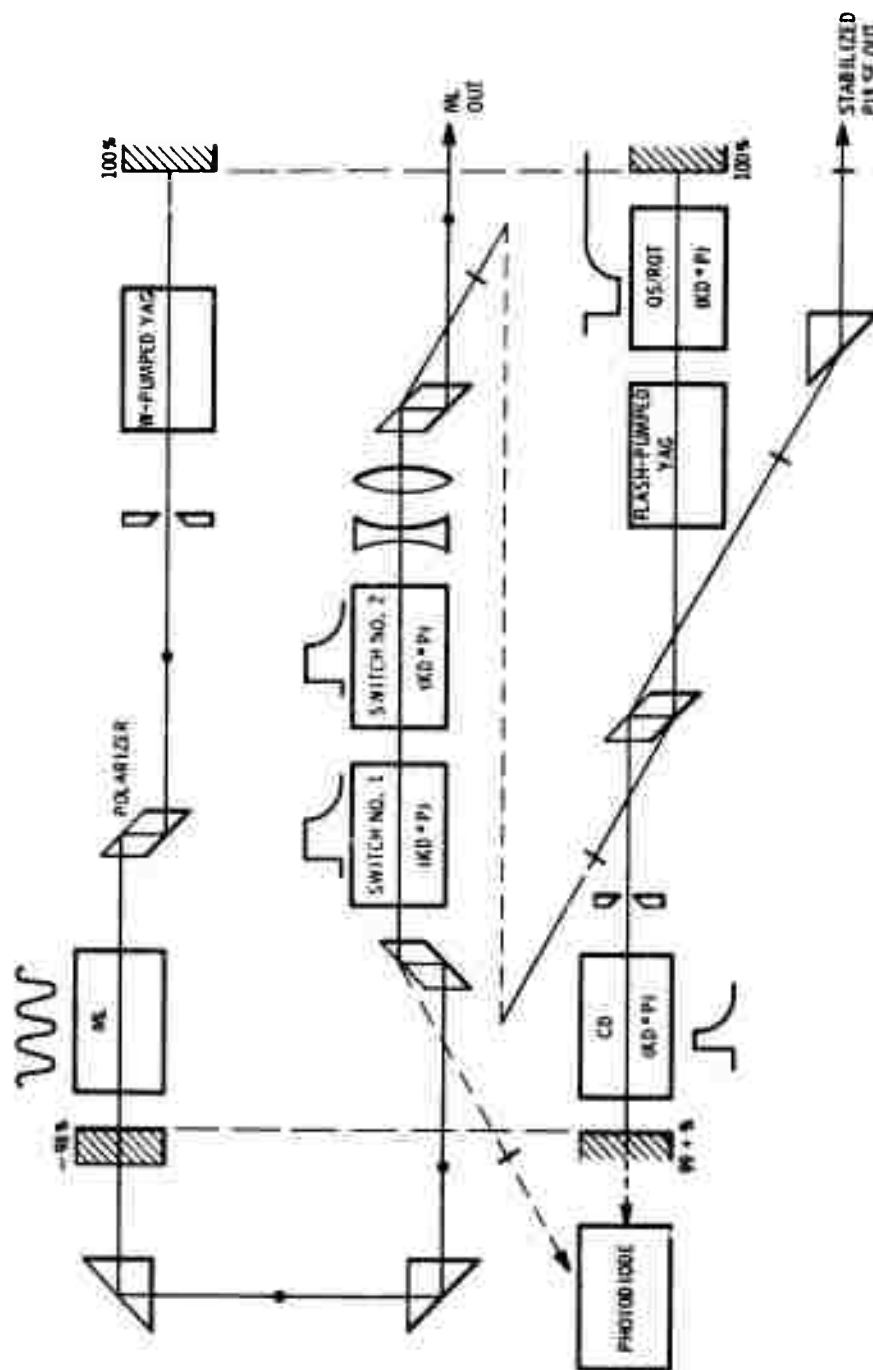
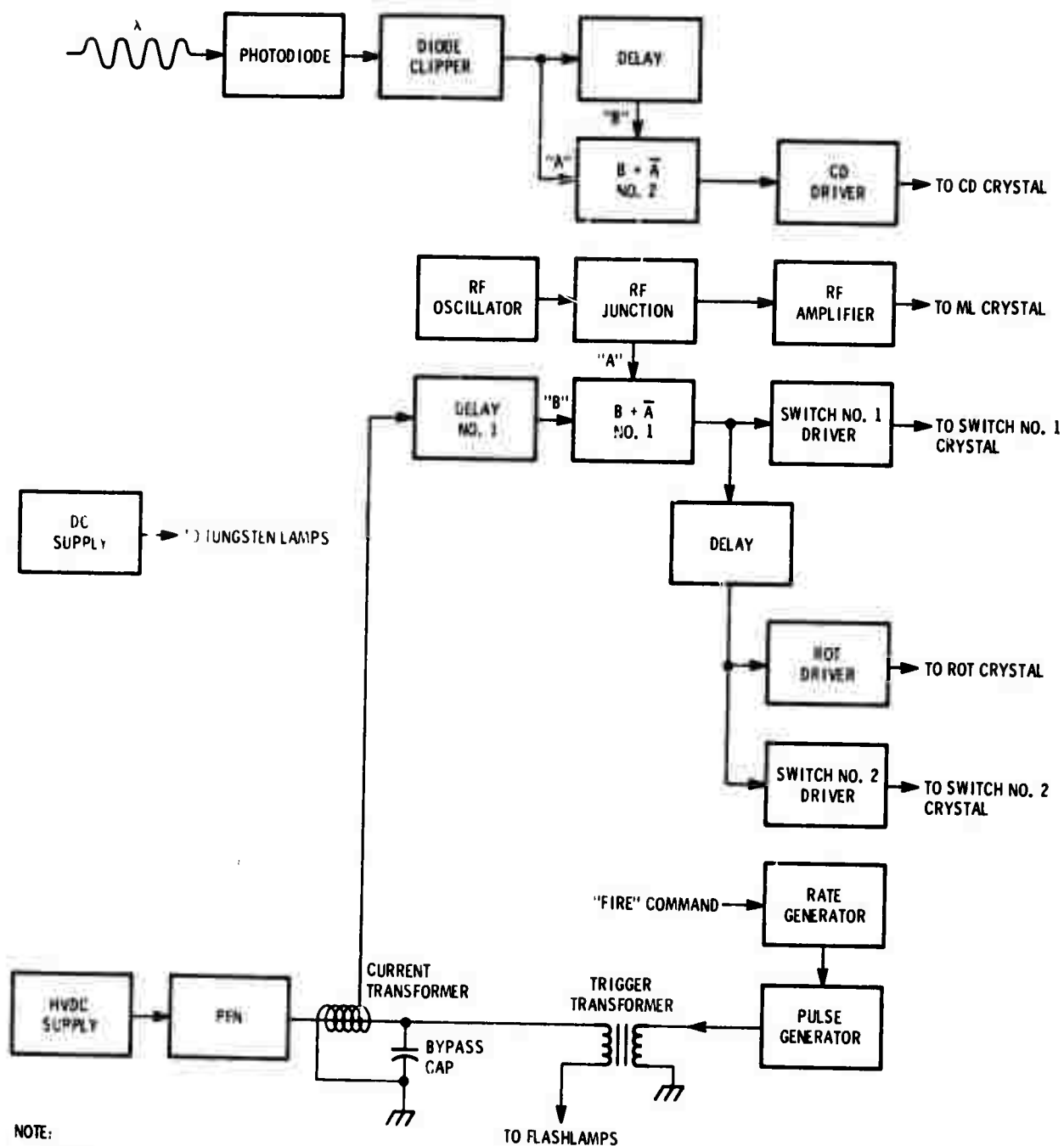


Figure 2.1 Optical Block Diagram



NOTE:

NOT SHOWN:
MISCELLANEOUS DC SUPPLIES
INTERLOCK CIRCUITRY
SHORT DELAYS FOR PROPER PHASING

Figure 2.2 Electronic Block Diagram

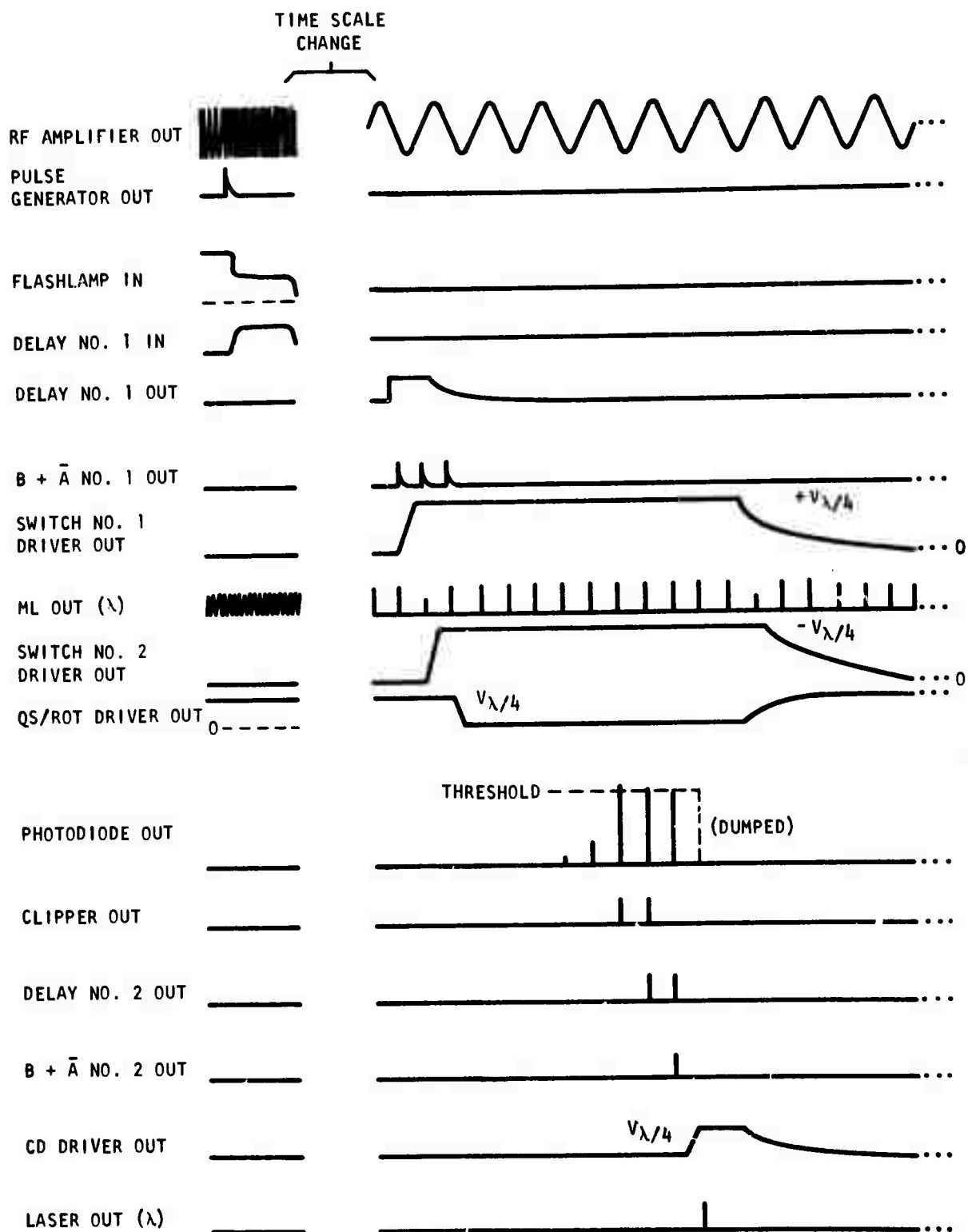


Figure 2.3 Timing Diagram

the photodiode, crosses and recrosses the electronic circuitry's threshold, the pulse is dumped. Since the pulse is dumped during its decay, its amplitude is selectable in steps which differ by the inherent cavity round-trip loss (scattering, absorption, mirror leakage) less the residual round-trip gain. The latter is variable simply by varying Delay No. 1 such that switching occurs during the appropriate portion of the end of the flashlamp pulse; hence, the net loss can be minimized, and therefore also the difference between amplitude steps.

We originally elected to use YALO rather than YAG as the laser material, because YALO has about twice the energy storage capability of YAG (Ref. 1) and, more important, does not suffer polarization loss due to thermally-induced birefringence (Ref. 2). YALO lases at $1.0645\text{ }\mu\text{m}$ (or $1.0795\text{ }\mu\text{m}$, depending on orientation and polarization), while YAG lases at $1.0641\text{ }\mu\text{m}$; the optical quality of selected YALO has been as good as that of YAG. We found experimentally that the lower gain and greater thermal focusing of YALO (as compared to YAG) rendered it marginal at best for use in the subsidiary oscillator. The subsidiary oscillator was therefore converted to YAG; fluorescence measurements indicated that the overlap of the YAG laser line with the YALO fluorescence band would be sufficient for the YALO power oscillator to be used with the YAG subsidiary oscillator. We found experimentally that this arrangement was marginal at best, however, and converted the power oscillator to YAG also. Under another program (sponsored by NASA/Goddard Space Flight Center) we have found that YALO amplifier performance does not conform to theoretical predictions based on oscillator measurements. Theory predicts that a YALO amplifier should produce twice the extractable energy of a YAG amplifier; experimentally, a YALO oscillator/YALO amplifier was distinctly inferior to a YAG oscillator/YAG amplifier. We do not yet know the source of the discrepancy between the experimental data and the theoretical predictions, but inhomogeneous broadening and YALO micro-quality are prime suspects. YALO of good optical quality is no longer available.

3. OPTOMECHANICAL DESIGN

3.1 SUBSIDIARY OSCILLATOR

The power level obtained from the subsidiary oscillator is not critical; hence we have chosen to use tungsten-iodine-quartz pump lamps for long life and low cost. The lamps are air-cooled (using a built-in blower), but the rod and pump cavity are water-cooled. Mirror and rod-end curvatures are selected to approximately maximize the TEM_{00} mode volume in the rod, and an aperture constrains oscillation to this mode.

The resonant cavity end plates (which are shared by the power oscillator) are supported on isolation-mounted Invar rods. The resonant cavity is passively stabilized against ambient temperature variations by locating each mirror at a point within its mirror mount such that thermal effects on the mirror mounts, the Invar supports, the mode-locking crystal, and the air path are mutually compensating (the laser rod temperature will be as stable as the city water supply temperature, which normally does not vary by more than a few $^{\circ}C$). Output stability is further enhanced by the modelocking technique, which provides a high effective modulation depth.

The $c/2L$ frequency of the resonant cavity is about 150 MHz. The fused silica acousto-optic loss modulator is driven by a 75 MHz sinusoidal voltage. Since the zero-loss times occur at the voltage zero-crossings, this technique provides high effective modulation with relatively simple and inexpensive components. This technique does not provide the lowest modulator insertion loss, but maximized output power is not required for this application.

3.2 POWER OSCILLATOR

Optomechanical design of the power oscillator is relatively simple, since beam geometry can be primarily determined by the subsidiary oscillator and the beam-expanding optics, and since passive stabilization of the resonant cavity is not particularly important. The power oscillator, as it is operated in this system, is essentially a regenerative amplifier.

The laser rod, pump cavity, and flashlamps are all water-cooled. The lamps of either oscillator may be changed easily and rapidly without disturbing the optical alignment of any part of the system.

3.3 ELECTRO-OPTICAL SWITCHES

The optical switches originally all used 45° z-cut KD*P crystals in dual-crystal transverse-field Pockels cells, with Fresnel reflections suppressed by an index-matching liquid. The sw. #1 and sw. #2 crystals comprised one matched pair, the QS and CD crystals comprised another, and the rot. crystals were a third matched pair. These switches suffered gradual but irreversible deterioration of their optical faces (and, ultimately, the bulk material) as a result of surface (and bulk) currents. Each switch now uses 0° -cut KD*P crystals in a dual-crystal longitudinal-field Pockels cell, with Fresnel reflections suppressed by index-matching liquid. Two crystals (optically in series, electrically in parallel) are used in each cell in order to reduce the required drive voltage to a level that can be switched within $2L/c \approx 6.6$ ns. Since the longitudinal-field configuration has no field across the optical faces, it is much more resistant to current-induced damage. The effect of the non-uniform retardation across the aperture (due to the ring electrodes) has not been noticeable in the laser output.

3.4 THE LASER CHASSIS

The mounts for all of the optical components except the mirrors are attached to a single baseplate. This baseplate is stiffened transversely by three rectangular bars (to which the adjustable mounting feet are attached) and by the chassis endplates, and longitudinally by two lengths of channel stock. The Invar rods that support the resonant cavity end plates are isolation-mounted to the channels, and the rigid dust-cover is mounted to the channels and the chassis endplates. Much of the plumbing (water, air, and electrical) is confined to the under side of the baseplate, for esthetic reasons.

The high-current components (see Section 4.1) are mounted in a separate enclosure that mates with the laser assembly. This permits a simpler, lighter cable assembly to be used between the control console and the rest of the system (see Figure 4.1), and eases the task of RFI suppression. This enclosure and the laser assembly are shown in Fig. 3.1.

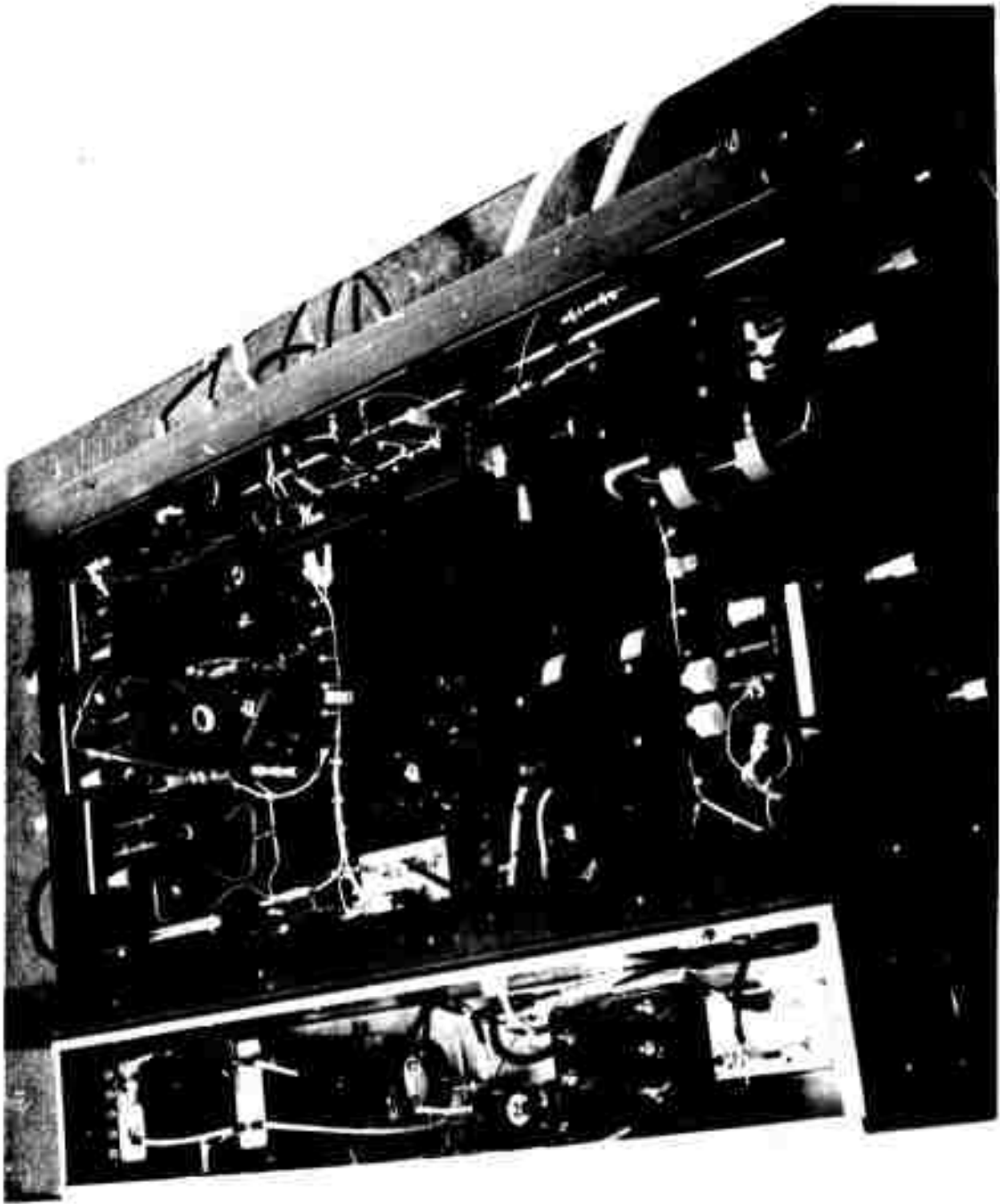


Fig. 3.1 Laser Chassis

4. ELECTRONIC DESIGN

This section will concisely discuss the electronic circuitry developed to perform the functions indicated on the block and timing diagrams in Fig. 2.2. The laser excitation is covered in 4.1, with important aspects of the RF circuitry being presented in 4.2. Sections 4.3 and 4.4 discuss the logic electronics and Pockels cell drive circuitry performance, respectively. Section 4.5 covers the system's control and protection features.

The lamp power supplies, Pockels cell power supply, control and interlock circuitry, and some of the RF circuitry are contained in the control console, shown in Fig. 4.1. The high current electronics are located in the enclosure associated with the laser chassis, and the remaining electronics are attached to the laser chassis.

4.1 LASER EXCITATION

The tungsten lamps are driven in parallel by a constant-voltage/current-limiting DC power supply. The lamps are rated at 1.0 kW each. The proper lamp envelope temperature is maintained by a built-in air-cooling system.

The flashlamps are driven in series by a double-mesh pulse-forming network (pfm) of critically-damped design (Ref. 4). The lamps are triggered by a series trigger transformer in order to ensure maximum triggering reliability and to provide additional protection against underdamped operation. The polarities of the power supply and trigger pulse are those recommended by the lamp manufacturer for maximized triggering reliability and lamp life (Ref. 5). Lamp life should exceed 10^6 shots with negligible output degradation at the design maximum of 20 J per lamp.

The pfm capacitors are pulse-charged by the charging power supply. This technique, based on a 1600 Hz inverter, allows voltage regulation to $\leq 2.5\%$. A built-in recharge delay allows time for lamp deionization, thus obviating lamp "hang-up" (or, "hold-on").

4.2 R.F. CIRCUITRY

An amplitude-and frequency-stable r.f. signal is used for two purposes in the system: 1) to drive the mode-locking modulator, and 2) to provide timing information for the logic circuitry. The signal is generated by



Fig. 4.1 Control Console

an internal 75 MHz solid state oscillator (for determination of the oscillator frequency, see Section 3.1). This unit is mechanically tunable from 60 - 84 MHz at a power output of +15 dbm, constant to 0.5 db from -30°C to $+70^{\circ}\text{C}$. Its frequency stability is $0.005\%/^{\circ}\text{C}$. DC power for the oscillator is +28 Vdc at 20 mA.

One portion of the oscillator output is amplified to a nominal 2 watt (+33 dbm) level by a solid state Sylvania-built r.f. amplifier. The schematic (furnished with the operation manual) utilizes a 2N4072 as a preamplifier and a 2N3961 as the power amplifier stage. Both the r.f. oscillator and its associated amplifier are physically contained in the System Control portion of the control chassis. Since the amplifier is a narrow-band design, the output stage must be re-tuned whenever the oscillator frequency is changed by more than 2 MHz. The DC power required is +28V at 300 mA.

4.3 LOGIC AND TIMING CIRCUITRY

The system's logic and timing circuitry are all contained within either the Delay 1 and Logic subassembly located on the System Control chassis, or in the Delay 2 subassembly located on the laser chassis.

The Delay 1 and Logic unit is activated by a signal received from a current monitor which senses the flash lamp current in the power oscillator. After a (nominal) 150 μs adjustable delay, a CA3028A connected as an AND opens and waits for a positive-going, voltage-zero-crossing from the RF oscillator. This condition, of course is satisfied once every rf cycle (at 75 MHz). At the coincidence of both input conditions, i.e., the first positive-going zero crossing of the 75 MHz RF, 150 μs after the start of current flow through the power amplifier laser flashlamp, the Delay 1 and Logic unit generates a 5V pulse which is delivered to the Pockels cell drivers associated with Switch No. 1, Switch No. 2, and Q-S/Rot. (see block diagram, Fig. 2.2). The coaxial cable lengths are such that: sw. #1 switches from zero to $+V_{\lambda/4}$ just before the selected pulse traverses it; sw. #2 switches from zero to $-V_{\lambda/4}$ just after the pulse traverses it; and QS/rot. switches from $V_{\lambda/4}$ to zero just after the pulse traverses it (twice - once in each direction).

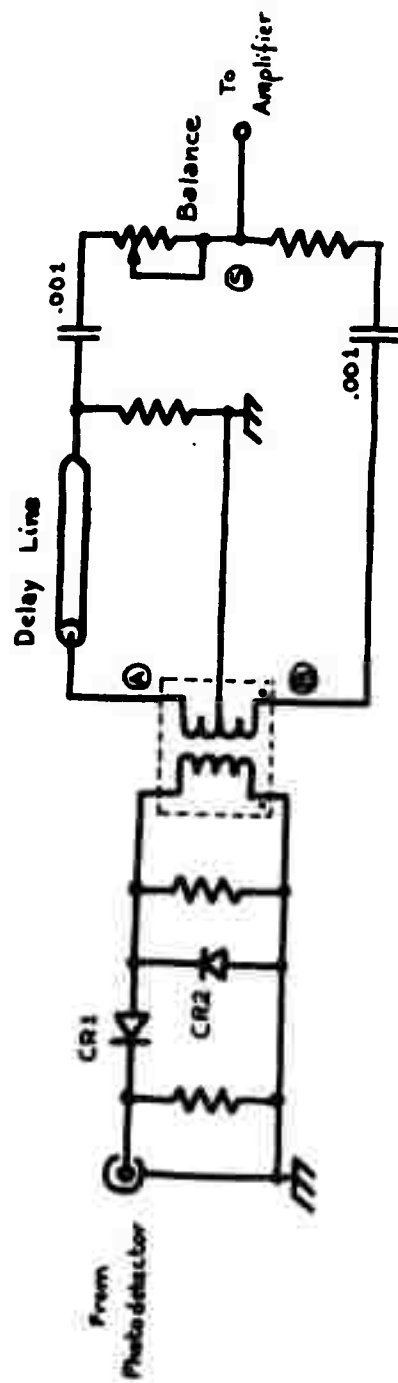


Fig. 4.2 Delay 2

The Cavity Dump driver is controlled by a command generated in the Delay 2 unit, the heart of which is shown in Fig. 4.2. The unit is completely enclosed in a 1.7" x 2.6" x 4.3" aluminum box, for RFI protection, and is mounted on the laser chassis.

End mirror leakage from the power amplifier cavity is directed via a fiber optic assembly to the active area of a Coherent Optics Model 32 avalanche photodetector. Its output is a negative voltage proportional to the input radiation pulse power. Since the pulse power in the cavity first increases rapidly and then decays, the photodetector output is a group of pulses, the first part of which increase in amplitude rapidly with the remainder decaying at a somewhat slower rate. Referring to Fig. 4.3, the input pulses from the photodetector are clipped to a constant height with CR2. By adjusting a symmetrical π attenuator between the photodetector and the CR1-CR2 diode input, the proper cavity peak power threshold may be selected. This adjustment is made with the complete laser package operating.

The constant height photodetector pulses spaced 6.7 ns apart (the cavity round trip time) are fed into a balanced transformer. The CR1-CR2 diode combination assures that the beginning and end of the pulse train correspond to crossing the threshold positively and negatively, respectively. Output (A) (equal in magnitude but opposite in polarity to that at (B) is delayed by 4.18 ft. of miniature coaxial cable - a delay of 6.7 ns. The cable output and output (B) are summed at (S). The net output at (S) is a pulse coincident with the positive crossing through threshold, and a pulse of opposite polarity occurring 6.7 ns after the negative crossing through threshold. This second pulse is amplified and delivered to the Cavity Dump driver through an appropriate length of cable.

These Sylvania-built circuits, the Delay 1 and Logic unit - and the Delay 2 unit, both require DC power of +28V, at 85 mA and 25 mA respectively.

4.4 POCKELS CELL DRIVE CIRCUITRY

A standard Pockels cell driver, Fig. 4.3, is used as the driver for Switch No. 1, Switch No. 2, Cavity Dump, and QS/Rot. (ref to Fig. 2.2). It is a proprietary design that will switch KD*P through 2 kV in <5 ns. The unit is driven with a +4 V logic pulse; it also has the capability to apply a 0 - 2000 Vdc bias to the crystal as required. The complete driver circuit schematic is included in the operation manual.

4.5 SYSTEM CONTROL AND PROTECTION CIRCUITRY

The PRF for the system is generated by the Rate Generator located in the System Control Console. It produces a continuously variable PRF from 8 to 30 pps, and has a manual "single shot" capability. The generator incorporates a unijunction transistor in a relaxation oscillator circuit. The controls for selecting the operating mode (Standby, Manual, Continuous), for controlling the PRF, and the single-shot push button, are all located on the Control Console front panel. Required dc power is +28 V at 30 mA.

Output from the Rate Generator is channelled to the Pulse Generator unit, located near the pulse forming network for the power oscillator flash-lamps. This assembly essentially amplifies the 6V pulse from the rate generator to a 600V pulse to drive the flashlamp trigger transformer. The technique is straightforward : discharge a capacitor, via an SCR, through the trigger transformer primary. Further explanation of the pulse forming network is given in Section 4.1.

DC power for the subsidiary laser oscillator, the Pockels cell drivers, and the power laser oscillator is provided by three separate commercially available supplies, an EMI SCR-120-20, a Del 2.5 RHPT-50-1, and an ILC PS1500, respectively. The system voltage (+28 Vdc) is provided by a Powermate UNI-88.

Prime power required for the entire Amplitude-Stabilized Pulsed Laser system is 3Ø, 60 Hz, 120V/208V, "WYE" connected. Total system input power will be approximately 4.7 KVA at about 13 amps per leg. The only other required system input is tapwater for cooling at nominal rate of 2.5 gpm.

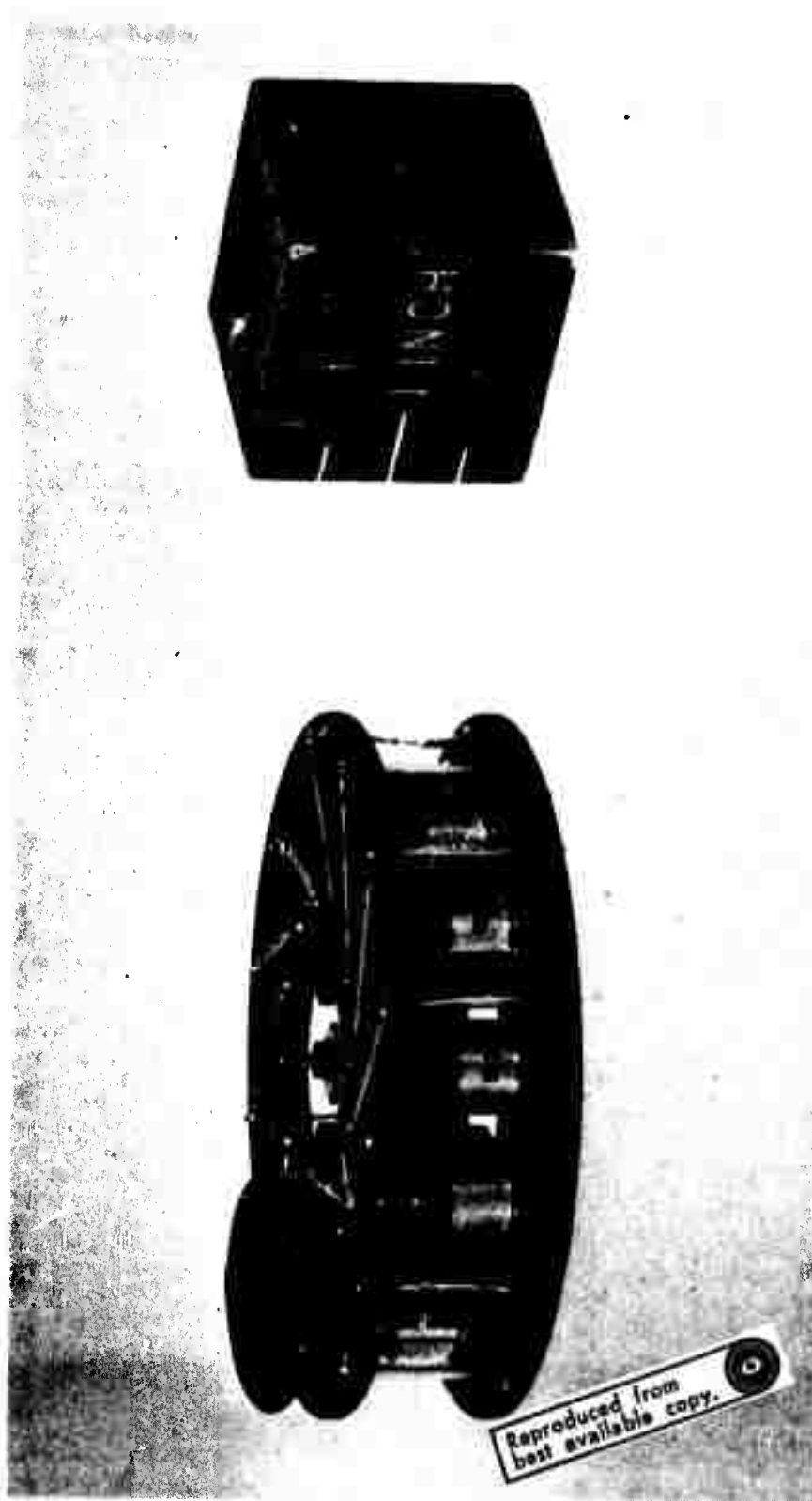


Figure 4-3. GTE Sylvania Pockels Cell Driver

The system is interlocked for both equipment and personnel protection and will cease operation if the console rear door is opened, or if the laser cover is removed or if the pulse-forming network cover is removed. (These interlocks may be overridden if it is mandatory that the system operate with a cover off or the door open.) In addition, if coolant water pressure is lost, or if a fault occurs within the cooling system (flow tube breakage, for example) the system will immediately shut down to avoid damage to other critical system components. The operator can, of course, stop the system at any time by merely opening the main power switch on the System Control front panel.

All of the above indicated methods of stopping system operation remove ac power from all but one component, that being the fan which provides cooling to the pump lamps in the subsidiary laser oscillator. (It runs for approximately 15 seconds after the system has been shut off.)

The Laser Chassis and the System Control Console may be operated up to 10 feet apart and an electrical cable assembly is provided as are the interconnecting coolant hoses.

5. EXPERIMENTAL RESULTS

During the acceptance tests, the parameters of the system were measured to be as follows:

wavelength : 1.064 μm
pulse rate : 8 to 30 pps
pulse duration : 72 to 108 ps FWHM (see text below)
pulse energy : 2.5 to 7.5 mJ (see text below)
amplitude fluctuation : 10% peak-to-peak range, with occasional
"missed" pulses (see text below)
integrated leakage : \lesssim 10% by circumstantial evidence (not directly
measured).
beam size : oval beam having equivalent circular diameter
(e^{-2} intensity) of 2.3 mm (\sim 0.5 m from the exit
port)
beam divergence : as corrected for wavefront curvature, 1.4
times the divergence of the equivalent
circular Gaussian beam.

The oval beam results from the near-Brewster's-angle exit and incidence of the beam at the oblique faces of the polarizers and the beam-correcting prism. It is easy to show that if the beam divergence from the subsidiary oscillator is δ , the beam divergence in the plane of the baseplate of the injected beam between the polarizers is approximately $n_e \delta$ and hence the difference between the major and minor diameters of the beam entering the aperture of the power oscillator is approximately $d_{\text{maj}} - d_{\text{min}} = (n_e - 1) \delta s$ where n_e is the extraordinary refractive index of calcite and $s \doteq 23$ cm is the separation between the polarizers. The same argument holds for the dumped beam between the polarizer and the beam-correcting prism. The major diameter of the oval beam can be mildly truncated by the aperture, but side lobes will be produced if it is severely truncated.

The aperture in the power oscillator is required in order to obviate Q-switched lasing from the rod annulus around the injected beam. The beam

cannot be expanded to fill the rod because self-focusing occurs and damages the rod (both bulk and surfaces). The self-focusing may be triggered by accumulated wavefront distortions, transverse gain variations, or uncompensated thermal focusing in the rod, or by the Fresnel pattern of the aperture (when a larger aperture, that is still smaller than the rod, is used). Nominally, the system operates below the measured self-focusing threshold for YAG (Ref. 6).

The 7.5-mJ output was the largest observed with pulses ~ 100 ps long. More typically, 6 mJ was observed for long periods. Efforts to increase the energy, by increasing the beam diameter and/or the gain, were uniformly unsuccessful. The system degraded to the 2.5-mJ level because of the accumulated damage. At this level, the amplitude-stabilization threshold circuitry did not work properly and was replaced by a delay generator.

Pulse duration was measured by a second-harmonic-generation (SHG) technique, Fig. 5.1 (References 7-10). An autocorrelation plot is shown in Fig. 5.2; the calibration is 120 ps/in if the pulse is Gaussian, and 85 ps/in if the pulse is Lorentzian (we have assumed the former). The plot must be symmetrical, and so the small hump marked "real" must occur on both sides of the main peak. The large hump marked "artifact" (which masks the second "real" hump) is due to bow in the guide rods for the carriage: at that point virtually all of the SHG is generated by the beam coming from the prism on the carriage, which is starting to pass through the ADP at an angle providing relatively efficient phase matching. This latter effect is due to the fact that the ADP is cut only approximately at the correct angles and therefore introduces unwanted and complicating effects due to the "extra" birefringence. Pulse duration measurements with a reflected-beam two-photon-fluorescence (TPF) apparatus gave pulse widths from ~ 35 ps to ~ 78 ps, somewhat shorter pulses than obtained from the SHG technique. There was some indication that the detector in the SHG experiment was on the verge of saturation, so that the shorter durations may be more correct. On the other hand, the TPF apparatus (kindly loaned us by the University of Maryland) utilized Polaroid film, so the pulse shapes given by the two methods could not accurately be compared. A typical TPF photo is shown in Fig. 5.3; the calibration is 222 ps/in if the pulse is Gaussian, and 157 ps/in if the pulse is Lorentzian.

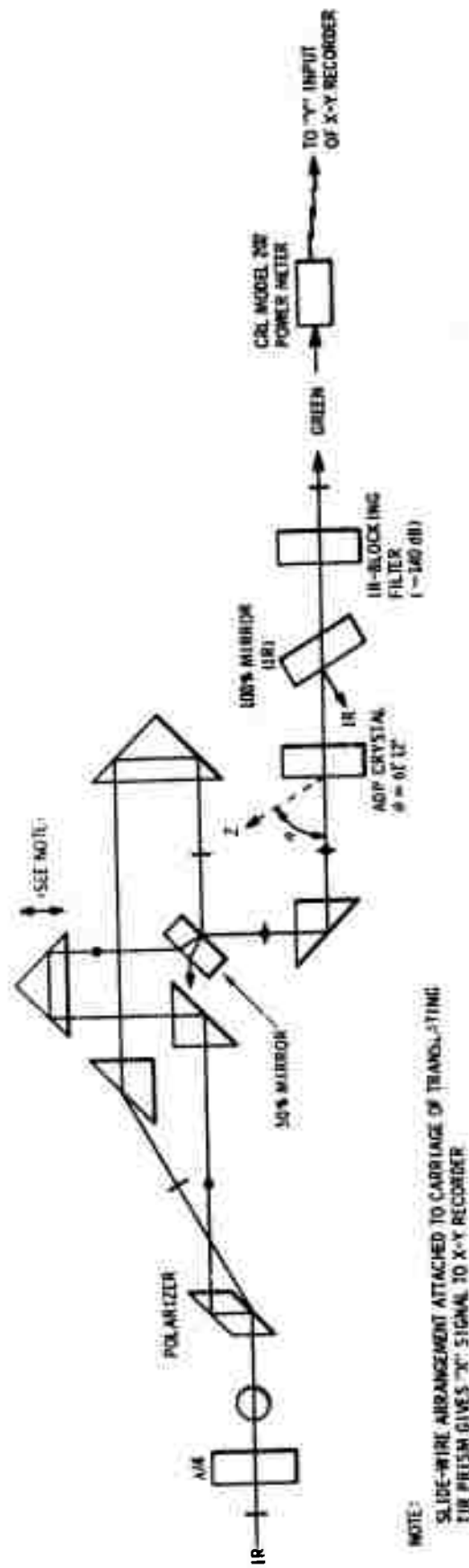


Figure 5.1 Pulse-Duration Experimental Setup

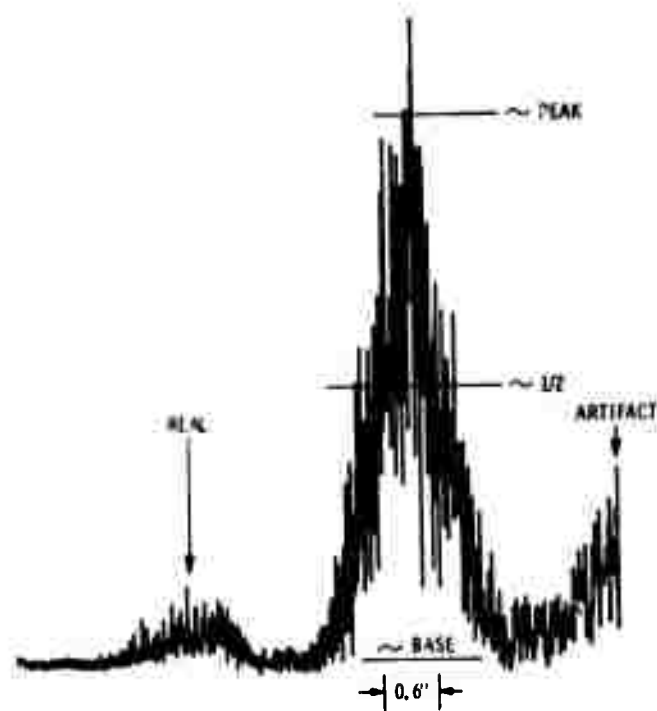


Figure 5.2 Pulse Autocorrelation Scan (SHG Technique)

A trace of the pulse injected from the subsidiary oscillator into the power oscillator is shown in Fig. 5.4; a Coherent Optics Model 32 High-Speed Light Detector was used with a Tektronix sampling'scope system consisting of a Type 351A Main Frame, a Type 3S2 Sampling Unit, an S-4 Sampling Head, and a Type 3T77 Sampling Sweep Unit. The S-4 has a specified risetime ≤ 25 ps and the Model 32 has a measured risetime of 81 (+22, -11) ps; hence the displayed pulse of 150 ps FWHM corresponds to an optical pulse of 91 to 119 ps FWHM. If anything, the injected pulse is shortened by the regenerative amplification.

Experiments with this laser indicate to us that pulse energies of ≥ 10 mJ in 100-ps pulses can be obtained from an oscillator of this type if very close attention is given to gain uniformity, compensation for thermal focusing, and interferometric quality of intracavity components. Self-focussing probably precludes pulse energies $\gtrsim 50$ mJ from being achieved in an oscillator of this type, however. Energies $\gg 10$ mJ will readily be obtained by the addition of amplifier stages.

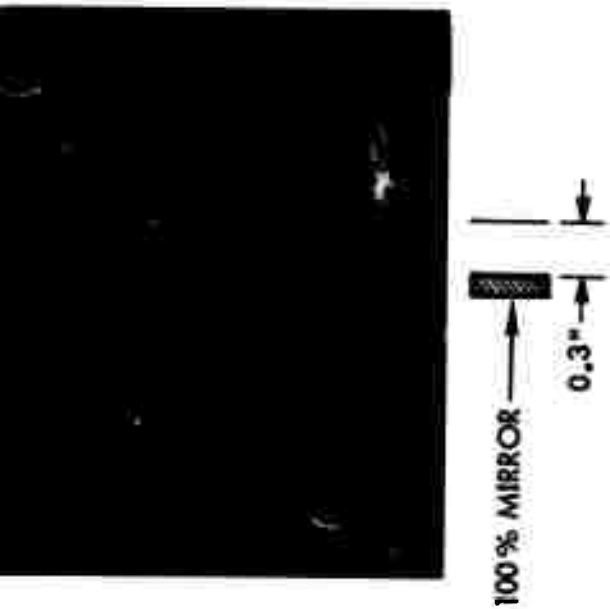


Figure 5.3 Reflected-Beam TPF Pulse Autocorrelation Photo

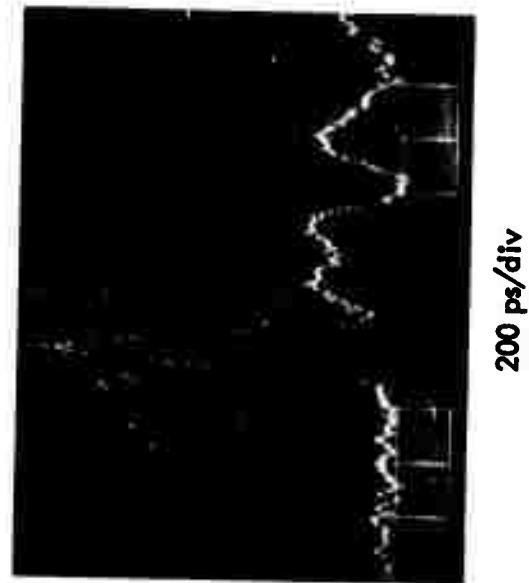


Figure 5.4 Trace of Injected Pulse

Reproduced from
best available copy.

6. RECOMMENDATIONS

For a number of potential applications of systems of the sort described above, higher pulse energy is very desirable. The most efficient and straightforward approach to this goal is to combine an oscillator such as this one with a chain of saturated amplifiers. The use of saturated amplifiers not only enhances the efficiency of the system, but it also improves the pulse-to-pulse amplitude stability available from the oscillator and negates the possibilities of significant after-pulsing and amplified target reflection.

The key to saturated amplifier design is the parameter $\beta E_{in}/A$, where β is the specific gain of the material ($\beta = \sigma/h\nu$, where σ is the laser ion cross section for stimulated emission and $h\nu$ is the energy of a laser photon), E_{in} is the energy of the radiation pulse to be amplified, and A is the effective amplifier cross-sectional area. If $E_{in}/A \geq \beta^{-1}$, the stored energy remaining in the amplifier after passage of the pulse will be less than $1/e$ of the stored energy just prior to passage of the pulse. We find that for YAG, $\beta^{-1} \approx 210 \text{ mJ/cm}^2$ @ $1.0641\mu\text{m}$ (Ref. 11); for YALO, $\beta^{-1} \approx 400 \text{ mJ/cm}^2$ @ $1.0645\mu\text{m}$ (References 1 and 11); and for Owens-Illinois ED-2 laser glass, $\beta^{-1} \approx 6.2 \text{ J/cm}^2$ @ $1.0623\mu\text{m}$ (from manufacturer's data).

For moderate amplified-pulse energies, YAG is presently the amplifier material of choice: for example, we calculate that two $1/4''$ - dia. YAG amplifier stages plus one of $3/8''$ - dia. will provide an output energy of approximately 1.4 J/pulse . To obtain much higher energies, additional amplifier stages utilizing Nd:glass can be used.

For pulse energies on the order of 100 mJ , another approach is worthy of attention. Our experience with this system, together with discussions with other people working in the subnanosecond-pulse field, indicate that a radical design change would result in pulse energies of this magnitude from a single oscillator. The output beam would approximate a truncated uniform plane wave, which is preferable to a Gaussian plane wave for most (if not all) applications; see Ref. 12.

7. REFERENCES

- 1) M. Bass and M. J. Weber, "Nd,Cr:YALO₃ Laser Tailored for High-Energy Q-Switched Operation", Appl. Phys. Lett. 17, 395-398 (1 Nov. 1970).
- 2) G. A. Massey, "Criterion for Selection of cw Laser Host Materials to Increase Available Power in the Fundamental Mode", Appl. Phys. Lett. 17, 213-215 (1 Sept. 1970).
- 3) Wm. D. Fountain, "Comments on: Transient Elastooptic Effects and Q-Switching Performance in Lithium Niobate and KD*P Pockels Cells", Appl. Opt. 10, 972 (Apr. 1971).
- 4) J. P. Markiewicz and J. L. Emmett, "Design of Flashlamp Driving Circuits", J. Quantum Electron. QE-2, 707-711 (Nov. 1966).
- 5) J. P. Moffat, Jr., ILC, private communication.
- 6) Wm. D. Fountain, unpublished
- 7) H. P. Weber, E. Mathieu, and K. P. Meyer, "Optical Mixing with Different Relative Polarizations of the Beams", J. Appl. Phys. 37, 3584-3586 (Aug. 1966).
- 8) J. A. Armstrong, "Measurement of Picosecond Laser Pulses", Appl. Phys. Letters 10, 16-18 (1 Jan. 1967).
- 9) H. P. Weber, "Method for Pulsewidth Measurement of Ultrashort Light Pulses Generated by Phase-Locked Lasers using Nonlinear Optics", J. Appl. Phys. 38, 2231-2234 (Apr. 1967).
- 10) A. J. DeMaria et al, "Picosecond Laser Pulses", Proc. IEEE 57, 2-25 (Jan. 1969).
- 11) T. Kushida, H. M. Marcos, and J. E. Geusic, "Laser Transition Cross Section and Fluorescence Branching Ratio for Nd³⁺ in Yttrium Aluminum Garnet", Phys. Rev. 167, 289-291 (10 Mar. 1968).
- 12) Wm. D. Fountain, "Far-Field Brightness of Amplified Laser Systems", submitted to Applied Optics.

8. GLOSSARY

ARPA	Advanced Research Projects Agency
CD	cavity-dump
KDP	KH_2PO_4
KD*P	KD_2PO_4
ML	mode-locking
ONR	Office of Naval Research
QS	Q switch
rot.	rotator
SHG	second-harmonic generation
sw.	switch
TPF	two-photon fluorescence
YAG	here, $\text{Nd:Y}_3\text{Al}_5\text{O}_{12}$
YALO	here, Cr,Nd:YAlO_3